ACCOUNTS of chemical research

Article

pubs.acs.org/accounts

Unconventional, Chemically Stable, and Soluble Two-Dimensional Angular Polycyclic Aromatic Hydrocarbons: From Molecular Design to Device Applications

Lei Zhang,[†] Yang Cao,[‡] Nicholas S. Colella,[†] Yong Liang,[‡] Jean-Luc Brédas,[∥] K. N. Houk,[‡,§] and Alejandro L. Briseno*[,†]

[†]Department of Polymer Science and Engineering, University of Massachusetts, Amherst, Massachusetts 01003, United States

[‡]Department of Chemistry and Biochemistry and [§]Department of Chemical and Biomolecular Engineering, University of California, Los Angeles, California 90095, United States

[∥]Division of Physical Sciences and Engineering, Solar & Photovoltaics Engineering Research Center, King Abdullah University of Science and Technology − KAUST, Thuwal 23955-6900, Kingdom of Saudi Arabia

CONSPECTUS: Polycyclic aromatic hydrocarbons (PAHs), consisting of laterally fused benzene rings, are among the most widely studied small-molecule organic semiconductors, with potential applications in organic field-effect transistors (OFETs) and organic photovoltaics (OPVs). Linear acenes, including tetracene, pentacene, and their derivatives, have received particular attention due to the synthetic flexibility in tuning their chemical structure and properties and to their high device performance. Unfortunately, longer acenes, which could exhibit even better performance, are susceptible to oxidation, photodegradation, and, in solar cells which contain fullerenes, Diels−Alder reactions. This Account highlights recent advances in the molecular design of two-dimensional (2-D) PAHs that combine device performance with environmental stability.

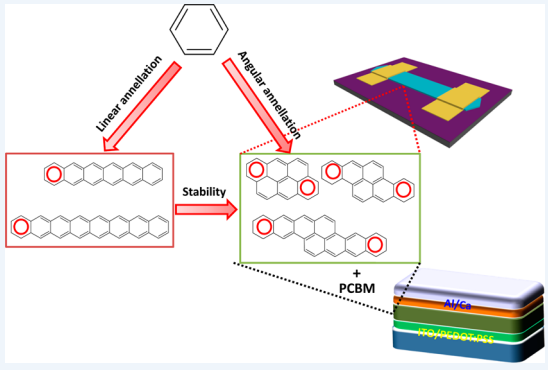

New synthetic techniques have been developed to create stable PAHs that extend conjugation in two dimensions. The stability of these novel compounds is consistent with Clar's sextet rule as the 2-D PAHs have greater numbers of sextets in their ground-state configuration than their linear analogues. The ionization potentials (IPs) of nonlinear acenes decrease more slowly with annellation in comparison to their linear counterparts. As a result, 2-D bistetracene derivatives that are composed of eight fused benzene rings are measured to be about 200 times more stable in chlorinated organic solvents than pentacene derivatives with only five fused rings.

Single crystals of the bistetracene derivatives have hole mobilities, measured in OFET configuration, up to 6.1 $cm^2 V^{-1} s^{-1}$, with remarkable I_{on}/I_{off} ratios of 10^7. The density functional theory (DFT) calculations can provide insight into the electronic structures at both molecular and material levels and to evaluate the main charge-transport parameters. The 2-D acenes with large aspect ratios and appropriate substituents have the potential to provide favorable interstack electronic interactions, and correspondingly high carrier mobilities.

In stark contrast to the 1-D acenes that form mono- and bis-adducts with fullerenes, 2-D PAHs show less reactivity with fullerenes. The geometry of 2-D PAHs plays a crucial role in determining both the barrier and the adduct stability. The reactivity and stability of the 2-D PAHs with regard to Diels−Alder reactions at different reactive sites were explained via DFT calculations of the reaction kinetics and of thermodynamics of reactions and simple Hückel molecular orbital considerations. Also, because of their increased stability in the presence of fullerenes, these compounds have been successfully used in OPVs.

The small-molecule semiconductors highlighted in this Account exhibit good charge-transport properties, comparable to those of traditional linear acenes, while being much more environmentally stable. These features have made these 2-D PAHs excellent molecules for fundamental research and device applications.

1. INTRODUCTION

The concept of aromaticity continues to be of central importance in physical organic chemistry for fundamental understanding of structure, stability, and chemical reactivity of polycyclic aromatic hydrocarbons (PAHs).[1−4] Several reviews have been devoted to both early and present research by leading investigators.[1−6] PAHs are currently among the most widely studied organic semiconductors due to their tailorability and the appealing characteristics of their electronic structure.[3] Particular attention has been paid to linear PAHs, which are composed of laterally fused benzene rings.[4,5] A wide variety of

Received: July 31, 2014
Published: December 2, 2014

 © 2014 American Chemical Society dx.doi.org/10.1021/ar500278w | Acc. Chem. Res. 2015, 48, 500−509

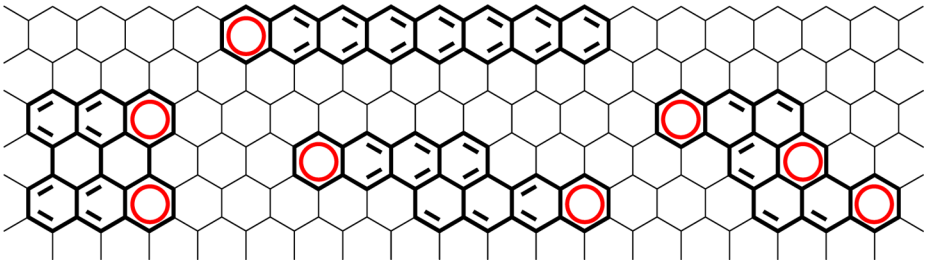

Figure 1. Schematic of graphene fragments illustrating a linear octacene with one Clar sextet and its angular isomers with various Clar sextets.

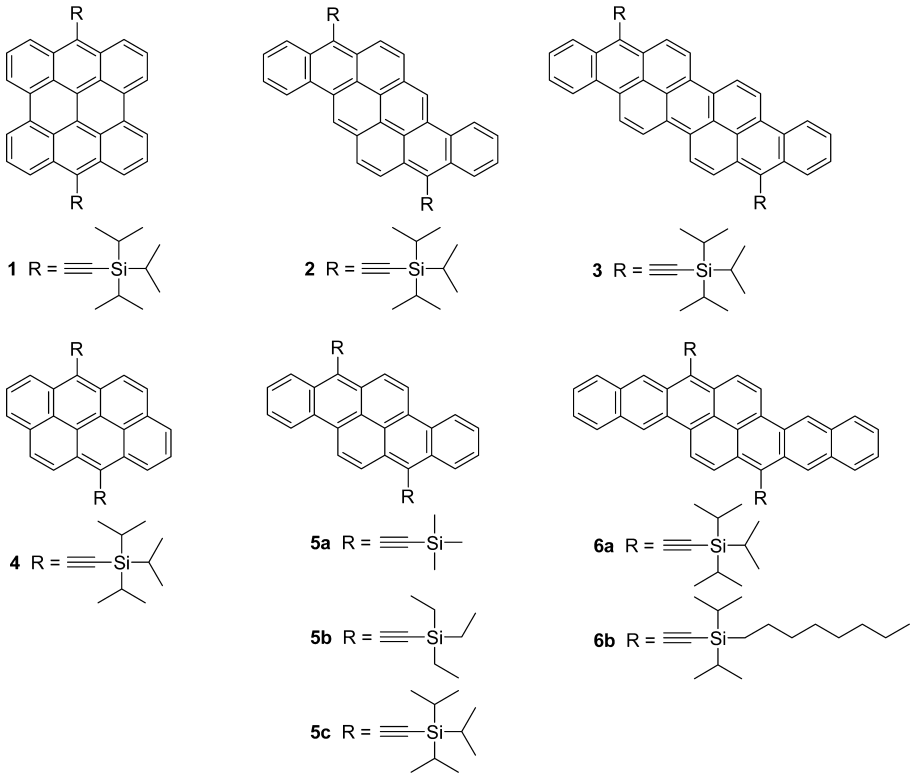

Figure 2. Molecular structures of 2-D polycyclic aromatic hydrocarbons with alkylsilylacetylene substituents.

linear acenes, such as tetracene, pentacene, and related derivatives, have been carefully designed and synthesized to produce highly desirable electronic properties, including remarkable charge-carrier mobilities.[6−8] Although increased conjugation length enhances electronic coupling and reduces reorganization energies in the solid state, which can lead to high charge-carrier mobilities,[5,9] linear acenes longer than five rings are not stable due to their low ionization potentials (IPs) and narrow band gaps.[10,11] It is in fact well-known that acenes become increasingly reactive as the number of rings increases, with the central ring being the most reactive.[12] As a result, the central rings in these molecules are susceptible to oxidation, photodegeneration, and Diels−Alder reactions.[13−15] Although some higher acenes can be stabilized by the addition of protecting bulky substituents,[16−20] many of the bulkier substituents disrupt the π-stacking motif and inhibit charge transport.

In general, the stability of large PAHs strongly depends on the mode of ring annellation and the topology of their π-electron systems.[21,22] From a theoretical viewpoint, the stability of PAHs can be qualitatively estimated by the application of the so-called Clar's sextet rule, which predicts the aromaticity of a benzenoid hydrocarbon on the basis of the maximum number of sextets of electrons in a system.[22,23] Thus, the stability of the acenes can be improved by increasing the number of aromatic Clar sextets.

One strategy is to annellate aromatic rings onto two neighboring rings, creating two-dimensional (2-D) acene analogues. Changing from a linear character of a condensed array (*peri*-condensed) to angular geometries (*cata*-condensed) results in at least two sextets, increasing the stability versus linear analogues which have only one sextet (Figure 1).[24] It should be noted that compounds with armchair edges are consistently found to have lower total energy and larger resonance energy than isomers with zigzag edges.[24] In particular, these small, well-defined, 2-D compounds that represent various fragments of graphene have large, planar π surfaces that can provide increased intermolecular surface overlap and effectively increase electron delocalization, potentially leading to enhanced transport properties.[3,25]

This Account focuses on the recent progress in this class of angular acene semiconductors and their applications in organic transistors and organic solar cells. The compounds considered here are modified by relatively bulky substituents, such as

dx.doi.org/10.1021/ar500278w | *Acc. Chem. Res.* 2015, 48, 500−509

Scheme 1. Synthetic Approach to Soluble "Bisoligoacene" Derivatives

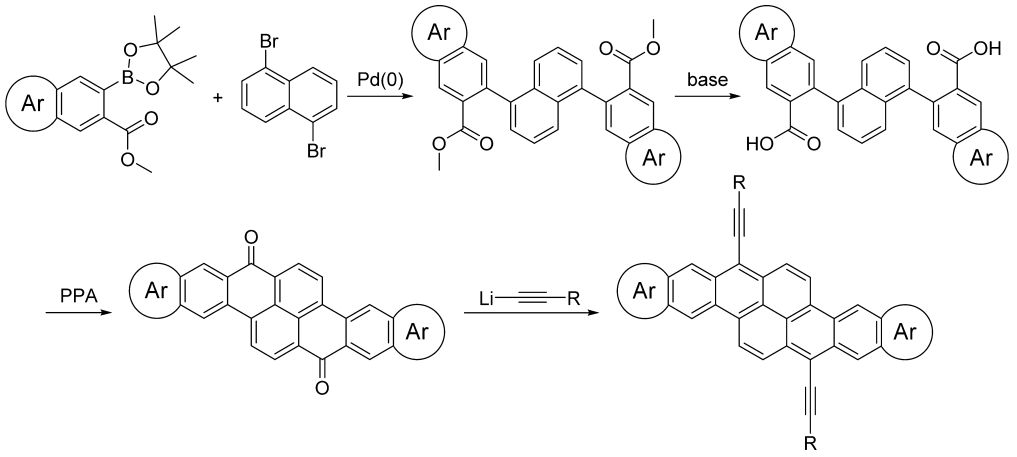

alkylsilylacetylenes, at the peri-position (Figure 2). It has been shown that this mode of substitution can avoid interrupting $\pi-\pi$ interactions while enhancing solubility and crystallinity, which are critical for high-performance devices.[5,6] In particular, density functional theory (DFT) calculations and experimental measurements have also shown that the bis-silylethynylation makes the disubstituted acenes much more stable, in particular with regard to oxidative degradation.[26,27] We also discuss the potential for Diels–Alder reactions between these compounds with fullerene derivatives, which reduces their potential applications in organic solar cells. Some molecules considered here, while not ideal for fabricating solar cells, should serve as model compounds for the development of large acenes that avoid reacting with fullerenes. This Account also illustrates the main features of the electronic structure of the 2-D PAHs and highlights the parameters that play important roles in device performance, such as crystal packing in the solid state.

2. MOLECULAR GEOMETRY AND ELECTRONIC STRUCTURE

2.1. Synthesis

Two-dimensional acene analogues have received significant attention as small molecular platforms to build up larger graphene subunits since the early 1990s.[28] Although "small graphene-like" molecules can be solubilized by the lateral attachment of flexible side chains, these side chains can disrupt the solid-state packing and result in fewer reactive sites for further functionalization. One prominent method for the synthesis of 2-D, soluble acenes is the nucleophilic addition of organometallic reagents with the corresponding quinones to form the alcohol derivatives, which is followed by a reductive aromatization to afford the desired products.[4] However, there is no efficient and general approach to condensed 2-D acene–quinone systems. This is due to the fact that the most common ring closures tend to proceed at the angular positions and molecules often exhibit extremely low solubility.[4] Although photocyclization is a powerful tool to access these quinones, this conventional route has been limited to only a few types of classical compounds.[29,30] We recently developed a new approach to synthesize "bistetracene" quinone.[31] The method takes advantage of a Pd-catalyzed cross-coupling reaction followed by an electrophilic aromatic substitution between acyl groups formed from the diacids with the 4- and 8-positions of naphthalene. The scope of this methodology can be extended to access various acene quinones and their derivatives by replacement of naphthalene derivatives with a wide range of aromatic systems (Scheme 1).

2.2. Electronic Properties and Stability

As mentioned earlier, the nature of the frontier energy levels and the molecular stability are among the most important properties for organic devices.[4−6] According to Clar's sextet rule, the shift from a linear acene to its angular analogue with the same number of aromatic rings is uniformly accompanied by a lower total energy and hence greater stability.[32] For instance, the IPs from cyclic voltammetry (CV) measurements of linear silylethyne-substituted hexacene derivatives that contain one sextet are on the order of 5.0 eV,[33] whereas the IPs of **4** and **5c**, which also contain six benzene rings but benefit from an additional sextet, are 5.4 eV.[34] This is also reflected in the absorption bands; the spectra of **4** and **5c** are blue-shifted by 0.83 eV compared to silylethyne-substituted hexacene. Although molecules **1** and **2** each consist of eight benzene rings, **1** contains two aromatic sextets while **2** has three sextets; as a result, the energy of the S_1 state of **2** is much larger than that of **1**.[34] These examples emphasize once more the PAHs exhibit extreme chemical stability with a high degree of angular or zigzag annelation.[4]

Importantly, while the optical gap and ionization potential of linear polyacenes rapidly decrease with the number of rings, these evolutions occur at a much slower rate for the angular analogues.[32] In general, there is a ∼100 nm bathochromic shift of the absorption maxima upon fusion of an additional aromatic ring onto the linear acene core.[6] In contrast, the UV absorption band of angular acenes changes slowly with an increasing number of rings; from **5c** to **6a**, there is a red-shift of only 145 nm (0.58 eV) following the fusion of two additional aromatic rings onto the acene core of **5c**. The IPs also decrease slowly from 5.45 to 5.11 eV.[34] By monitoring the absorption spectra of **6a** and pentacene under identical conditions (in chloroform), we found that **6a** has a half-life of 4 days, which points to a stability around 200 times larger than pentacene.[31] These results confirm that angular acenes are significantly more stable toward oxygen and light because of their lower oxidation potentials, which is critical for the development of stable devices.

2.3. Diels–Alder Reactivity with Fullerene Derivatives

Another fundamental problem regarding the chemical stability of PAH system is Diels–Alder (DA) reactions with fullerene

dx.doi.org/10.1021/ar500278w | Acc. Chem. Res. 2015, 48, 500−509

Table 1. CPCM($CHCl_3$)-M06-2X/6-31G(d)//M06-2X/3-21G*-Computed Activation Free Energies (ΔG_{act}, in kcal/mol) and Reaction Free Energies (ΔG_{rxn}, in kcal/mol) for the DA Reactions of the [6,6] Double Bond of C_{60} with Pentacene, Bistetracene, and Their Trimethylsilylethynyl-Substituted Derivatives

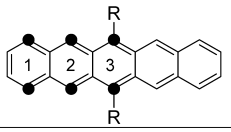

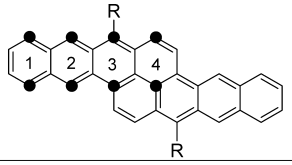

	R = H, pentacene (PT)			R = H, bistetracene (BT)			
site	1	2	3	1	2	3	4
ΔG_{act}	29.9	19.1	17.6	31.4	22.1	23.1	37.1
ΔG_{rxn}	4.3	-14.3	-18.6	7.0	-8.3	2.2	27.4
	R = trimethylsilylethynyl, TMS-PT			R = trimethylsilylethynyl, TMS-BT			
site	1	2	3	1	2	3	4
ΔG_{act}	29.6	19.8	16.8	33.6	23.4	25.9	39.8
ΔG_{rxn}	4.8	-13.0	-8.7	7.9	-7.3	8.4	29.5

derivatives, as linear acenes rapidly undergo DA reactions with fullerene derivatives in solution to form mono- and bis-adducts.[4] For example, the C═C bond on [60]fullerene (C_{60}) reacts with the central 6,13-carbons on pentacene and gives a symmetric monoadduct. For 6,13-disubstituted pentacenes, C_{60} reacts with pentacene at 5,14- and 7,12-positions to form mono- or bis-fullerene-pentacene adducts.[35] These adducts lead to ineffective photoinduced charge generation and separation.[36]

We have reported DFT calculations of the Diels−Alder (DA) reactions of pentacene (PT), 6,13-bis(2-trimethylsilylethynyl)-pentacene (TMS-PT), bistetracene (BT), and 8,17-bis(2-trimethylsilylethynyl)bistetracene (TMS-BT) with the [6,6] double bond of C_{60} (Table 1).[37] The introduction of the bulky silylethynyl substituents does not have a significant effect on reactivity, but influences the corresponding product stability substantially. The DA reaction on site 3 of PT is favored both kinetically, with the lowest barrier of 17.6 kcal/mol, and thermodynamically, with the most exergonic product of −18.6 kcal/mol (Table 1). This is consistent with the experimental result that the DA reaction of pentacene and fullerene occurs rapidly across the central 6,13-carbons to form a symmetric monoadduct.[35] The addition of trimethylsilylethynyl groups at the 6,13-positions lowers the activation free energy slightly, to 16.8 kcal/mol, and thus the DA reaction is still kinetically favored. Our calculations predicted that the monoadduct across site 3 should be observed under kinetically controlled reaction conditions. However, the steric repulsion between the bulky substituents and C_{60} significantly destabilizes the DA product as compared to the unsubstituted PT. This repulsion manifests in the longer (1.60 versus 1.58 Å, Figure 3) C−C bonds of the product. Because of these effects, the DA reaction of TMS-PT was predicted to be thermodynamically more favorable at site 2 in contrast to PT. These computational predictions (Figure 3) were later validated by monitoring the reaction of TIPS-PT and C_{60} via ^{1}H NMR.[37] The monoadduct on site 3 was formed in the first 10 min at room temperature but disappeared after a substantial reaction time (24 h in refluxing CS_2), and then the monoadduct across diene site 2 became the dominant product.

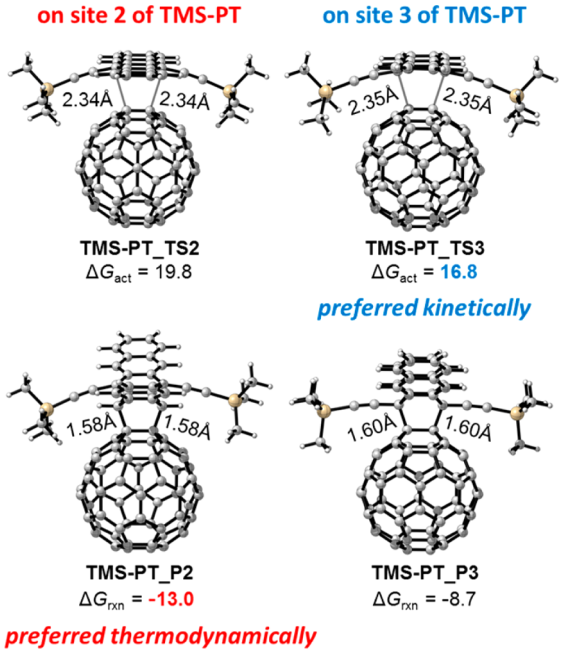

Figure 3. Computed free energies and structures for the C_{60}-TMS-PT DA reactions.

The activation free energies for the DA reactions of the four diene sites of BT and TMS-BT are similar (Table 1). Site 2 has the lowest barriers and is the only site with exergonic adduct formation.

The effects of additional fused aromatic rings were assessed through comparing the TMS-PT and TMS-BT systems. As shown in Table 1, the lowest DA activation free energies for TMS-PT and TMS-BT are 16.8 and 23.4 kcal/mol, respectively. On the basis of the free energy difference of 6.6 kcal/mol, the rate of the DA reaction of [60]fullerene with TMS-BT was predicted to be 70 000 times slower than that with TMS-PT at 25 °C. This accounts for the experimental observations.[37] The reaction of TIPS-PT with [6,6]-phenyl-

dx.doi.org/10.1021/ar500278w | Acc. Chem. Res. 2015, 48, 500−509

C_{61}-butyric acid methyl ester (PCBM) proceeds within a few minutes after mixture. In contrast, the reaction between TIPS-BT and PCBM is much slower, with almost no observable change in the first 36 h.

We also found that simple Hückel molecular orbital (HMO) calculations can give semiquantitative predictions of adduct stabilities. The localization energies (E_L) of different diene sites in a series of PAHs were computed with HMO. For the DA reactions of seven reaction sites in PT and BT (Table 1), Figure 4 shows a good correlation of DFT reaction free energies versus

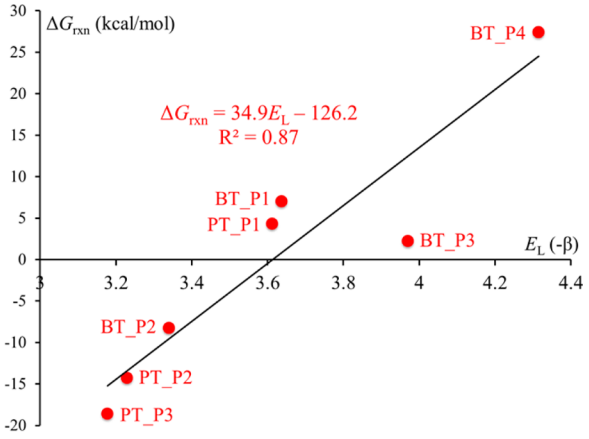

Figure 4. Correlation between HMO localization energies E_L and DFT reaction free energies of DA reactions on seven reaction sites in PT and BT.

HMO localization energies. This indicates that the loss of aromaticity mainly contributes to the reactivity of diene sites in PAHs.

We have applied the HMO calculations to a wider range of angular acenes (Figure 5), which could have better performance in organic devices. The linear equation in Figure 4 indicates that the HMO localization energy E_L of 3.6 corresponds to a reaction free energy of around 0 kcal/mol. Only reaction sites with E_L lower than 3.6 would be considered to be reactive in DA reactions with fullerene. The E_L values of various sites of 10 molecules are shown in Figure 5 with reactive sites (E_L < 3.6) marked in red. Based on the linear equation in Figure 4 and their E_L values, the reaction free energies can also be derived. The reaction free energies were also calculated from DFT methods to confirm this correlation. By comparing these two sets of data, we found that the differences for 6 reactive sites are in the range of 3.8 to −2.4 kcal/mol.[37] Therefore, the simple HMO method provides reliable estimations of the reactivities of different diene sites in various PAHs for DA reactions with fullerenes.

3. MOLECULAR GEOMETRY AND DEVICE PERFORMANCE

3.1. Crystal Packing in the Solid State

The isotropic nature of some of the 2-D molecules has a large effect on their crystal packing as energetically favorable π-stacking is the main driving force in the crystallization of these systems.[38,39] Although it remains very difficult to predict the packing arrangement of the PAHs as a function of different geometric features and substituents, it is worth noting that molecules which approximate a disk shape more easily form one-dimensional, close-to-cofacial packing in the solid state.[38−40] Typical examples are compounds **1** and **4**, which have an aspect ratio (length versus width) close to 1: the compounds crystallize with close-to-cofacial $\pi-\pi$ packing (Figure 6).[34] When the compounds have a large aspect ratio, the $\pi-\pi$ interactions predominately occur along the long axis (Figure 6A). It should also be noted that molecules with a small aspect ratio, resulting in "zig-zag" edges as seen in compounds **2** and **3**, can provide enough volume for the molecules to rotate and reorient to form slipped $\pi-\pi$ stacking; this results in a decrease in $\pi-\pi$ surface (spatial) overlap but not necessarily in wave function overlap which is the key parameter with regard to charge transport.[41]

Packing in the solid state can be further tailored by the selection of the silylethynyl functional group. In comparing **6a**, which has a 1-D slipped stack packing with poor interstack electronic coupling, to **6b**, which packs more tightly due to the attractive dispersive forces between the linear octyl chains, the dimensionality of the electronic structure is effectively increased, leading to enhanced transport properties.[31] By changing the substituents to smaller groups, the packing motifs changed to a sandwich herringbone packing, or one-dimensional π-stacked arrangements.[42,43] The change in packing motif with the size of the substituent is in accordance with the

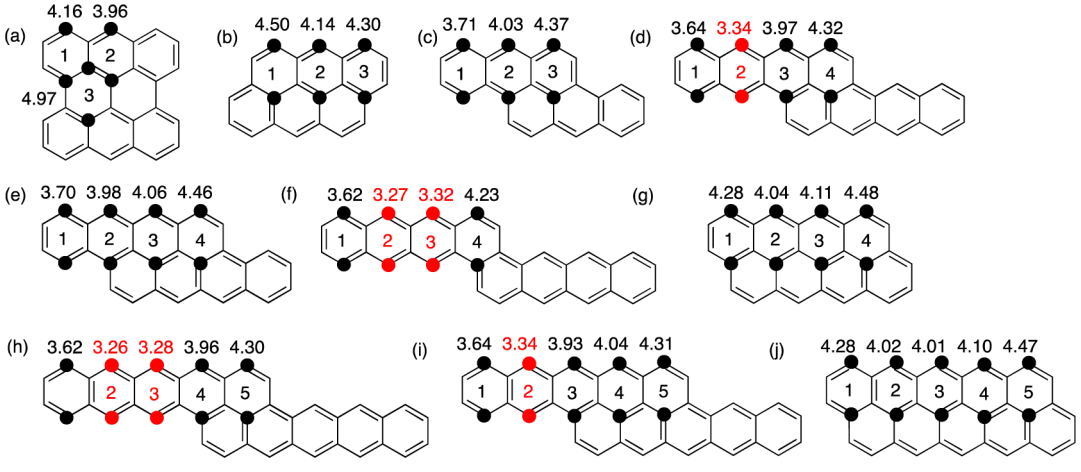

Figure 5. Structures of angular acenes with large aspect ratios as potential high-performance organic semiconductors and their HMO 1,4-localization energies (in units of $-\beta$).

dx.doi.org/10.1021/ar500278w | Acc. Chem. Res. 2015, 48, 500−509

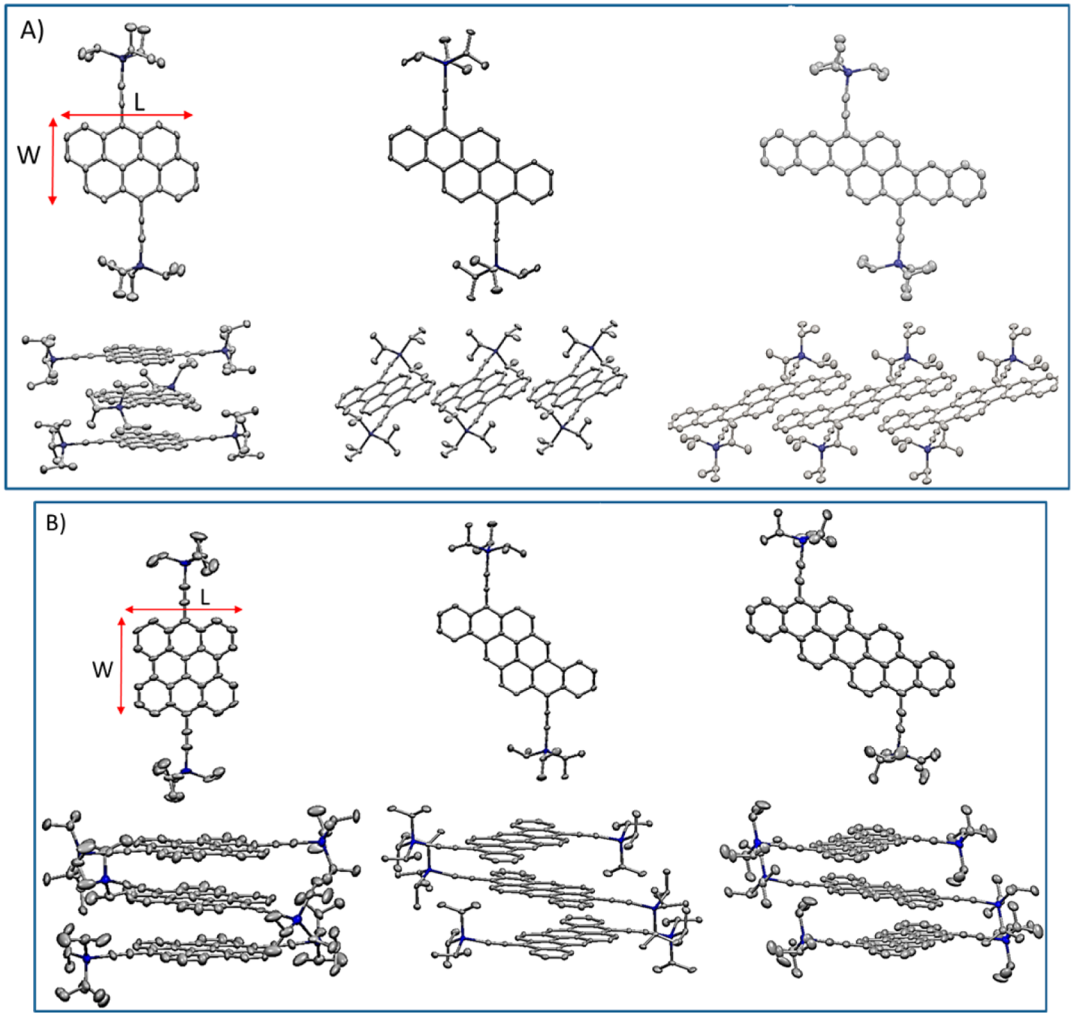

Figure 6. Crystal evolution in one column with different molecular geometries. (A) From cofacial $\pi-\pi$ stacking to slipped 1-D packing along the long axis with increasing length of narrow molecules. (B) From cofacial $\pi-\pi$ stacking slipped 1-D packing along short axis with increasing length of wide molecules.

model developed for pentacene derivatives.[5,6] Another important consideration is the substitution position. When the solubilizing groups are closer to the center of the PAHs, the molecules exhibit an offset $\pi-\pi$ stacking with more π surface overlap. From **5c** to **6a**, with the addition of another benzene ring on the periphery, the amount of $\pi-\pi$ overlap along the long axis significantly increased from 5.64 to 20.36 Å^2.[31,34]

3.2. Transfer Integrals and Effective Masses

The rich physics associated with charge transport in organic molecular semiconductors, such as acenes and their derivatives, originates in the interplay between the strength of the electronic couplings among adjacent molecules and the strength of the electron−vibration (phonon) couplings.[41,44] In the presence of minimal disorder (as in a single crystal), a band regime of transport with delocalized charge carriers can be achieved when the electron couplings are large (~100 meV and higher) and markedly greater than the electron−vibration couplings (which, in the context of Marcus theory of electron transfer, correspond to the combination of intramolecular and intermolecular reorganization energies).[44] Mobilities can then be expected to be significantly larger than ~1 cm^2 V^{-1} s^{-1}, and charge-carrier effective masses become a relevant parameter to describe transport.

For the PAHs shown in Figure 2, the calculated values of the largest transfer integrals for holes range from 44 to 194 meV. These values are larger than that estimated at a similar level of theory for TIPS-pentacene, which has a hole transfer integral of ~30 meV. In contrast, the values of transfer integrals for electrons are in the range of 25−140 meV, smaller than the value of 180 meV estimated for TIPS-pentacene.[34] Although compound **1** presents significant electronic coupling for both holes and electrons, with values up to 200 meV, the 1-D stacks are well separated by the TIPS groups, precluding electronic interactions between adjacent stacks. The stacks in compound **4**, **5c**, and **6a** are similarly isolated.[31,34] Interestingly, in **6b**, the electronic coupling along the $\pi-\pi$ stacks is characterized by two transfer integrals due to the two translationally inequivalent molecules in the unit cell. Additionally, unlike the case of **6a**, non-negligible electronic couplings were found between stacks in **6b**, 14 and 4 meV for holes and electrons, respectively.[31] This highlights the importance of selecting appropriate side groups to maximize the overall charge transport in organic semiconductors. In a band regime, charge mobility is inversely proportional to the effective mass of the charge carriers, and small effective masses for holes and electrons are also found along the $\pi-\pi$ stacking direction, while the effective masses in other directions are an order of magnitude larger. Particularly

dx.doi.org/10.1021/ar500278w | Acc. Chem. Res. 2015, 48, 500−509

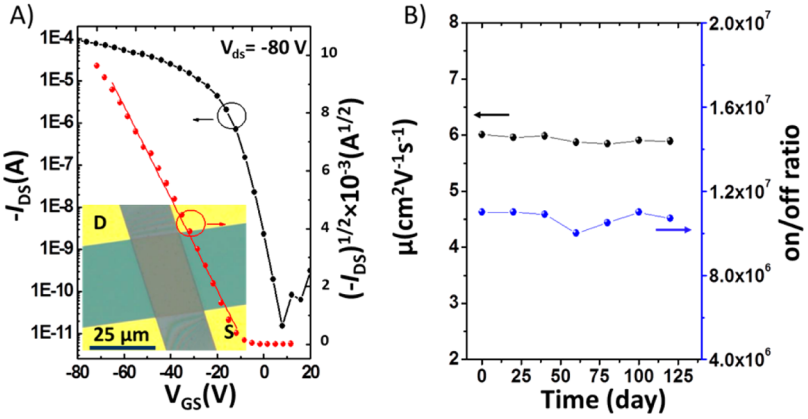

Figure 7. (A) Transfer characteristics in the saturated region of **6b** and (B) device stability test over several months.

small effective masses, from 0.69 to 1.07m_0, are found for holes in **5c**, **6a**, and **6b**, which have larger aspect ratios.[31,34] In the systems with small aspect ratios, the effective masses of both electrons and holes are roughly 2−3.0m_0. For compound **4** with close-to-cofacial $\pi-\pi$ stacking, the effective mass for holes is as large as 7.32m_0, which again underlines the difference between wave function overlap and spatial overlap.[34]

3.3. OFET Performance

The hole mobility in single crystals of acenes increases with the number of aromatic rings, with Batlogg and co-workers reporting values at room temperature going from 0.02 cm^2 V^{-1} s^{-1} for anthracene to 0.4 cm^2 V^{-1} s^{-1} for tetracene and 1.4 cm^2 V^{-1} s^{-1} for pentacene.[45] When the number of benzene rings in acenes is more than five, such as hexacene, heptacene, and beyond, the materials are generally not sufficiently stable to be characterized in devices.[9] One exception, reported in 2012, is a single-crystal transistor of hexacene fabricated through a physical vapor-transport (PVT) method from a monoketone precursor by Watanabe et al.[46] This crystal exhibits a hole mobility up to 4.3 cm^2 V^{-1} s^{-1}. However, the performance still gradually decays even under nitrogen atmosphere. Although significant progress has been made in the development of soluble higher acenes, their application for devices and properties in the solid state are almost completely unexplored.

As highlighted earlier, the increased number of Clar sextets present in 2-D PAHs results in significantly enhanced stability. In fact, while the 2-D PAHs demonstrated drastically better stability than linear acenes with a comparable number of aromatic rings, it should be noted that **6a** exhibited better stability (about four times the half-life) than that of even TIPS-pentacene under the same conditions.[31] As a result, relatively environmentally stable devices can be produced from these molecules. The average mobility measured for **6b** is ∼3.9 cm^2 V^{-1} s^{-1}, with a maximum mobility of 6.1 cm^2 V^{-1} s^{-1} (Figure 7), which is higher than that of materials with similar 2-D packing motifs such as TIPS-pentacene.[5,6] The average performance of **6a** devices is 0.28 cm^2 V^{-1} s^{-1} (best mobility of 0.4 cm^2 V^{-1} s^{-1}), which is likely related to the decreased interstack interactions. In a way similar to the decrease in mobility between pentacene and tetracene, the hole mobility in single-crystal transistors fabricated from **5c** falls to 0.1 cm^2 V^{-1} s^{-1},[34] which is lower than that of **6a** (Table 2).[31]

The aforementioned importance of interstack coupling is even more crucial when considering devices based on thin films of PAHs, as these contain high numbers of morphological

Table 2. Summary of the OFET Device Structure, Field-Effect Mobilities (μ), I_{on}/I_{off} Ratios, and Threshold Voltages (V_T) Based on 2-D PAHs[a]

compd	device structure	μ (cm^2 V^{-1} s^{-1})	I_{on}/I_{off}	V_T (V)	ref
3	TC/single crystal	(4.5 ± 2) × 10^{-3}	10^3	−5.0	34
4	TC/single crystal	(2.5 ± 1) × 10^{-5}	10^3	−10.0	34
5a	TC/thin film	1.17 ± 0.12	10^6		43
5b	BC/thin film[b]	1.6 × 10^{-3}			42
5c	BC/thin film[b]	1.0 × 10^{-3}			42
5c	TC/single crystal	(7.5 ± 1) × 10^{-2}	10^3	−2.8	34
6a	BC/single crystal	0.28 ± 0.10	10^6	6.0	31
6b	BC/single crystal	3.88 ± 1.40	10^7	−5.0	31

[a]TC = top contact, BC = bottom contact source and drain electrodes. All devices measured in a bottom-gate geometry. [b]Device statistics not reported.

defects.[41,44] An illustration of this phenomenon is observed when comparing compounds **5a** and **5c**. The mobilities of single-crystal transistors of **5c** are 2 orders of magnitude larger than that of thin films, which have mobilities on the order of 10^{-3} cm^2 V^{-1} s^{-1}.[42] While **5a** also has a crystal structure with 1-D packing, mobilities in thin-film transistors are larger than 1 cm^2 V^{-1} s^{-1}, due to significant electronic interactions between adjacent stacks, leading to highly crystalline film with large crystal grains.[43] Among the series, single-crystal transistors of compound **4** show the lowest mobilities, on the order of approximately 10^{-5} cm^2 V^{-1} s^{-1}; this low mobility can be attributed to defects and, as discussed above, to poor electronic interactions between different stacks.[34] These results show that 2-D acenes with large aspect ratios and appropriate substituents have the potential to provide 2-D packing with favorable interstack electronic interactions, and correspondingly high carrier mobilities.

3.4. Film Morphology and OPV Performance

Due to the high reactivity between acenes and fullerene derivatives, the use of these compounds in bulk heterojunction solar cells has been limited.[36] In 2009, Winzenberg and co-workers reported soluble chrysene derivatives as donors in solution-processed solar cells.[47] Devices fabricated from blends of **5c** and PCBM display an open-circuit voltage (V_{OC}) of 0.83 V, short-circuit current (J_{SC}) of 6.55 mA/cm^2, fill factor (FF) of 0.41, and power conversion efficiency (PCE) of 2.2%. This type of material has been also successfully used in thermally evaporated bilayer solar cells with C_{60} as acceptor, with the best PCE on the order of 2.2% as well.[48] Recently, compound **4**

dx.doi.org/10.1021/ar500278w | Acc. Chem. Res. 2015, 48, 500−509

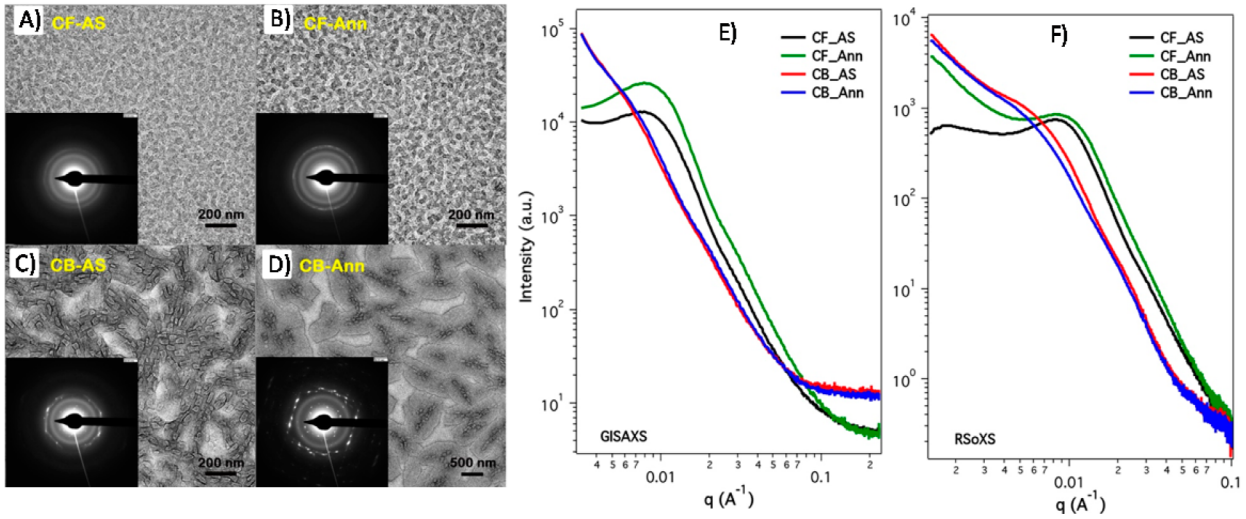

Figure 8. Transmission electron microscopy images with corresponding electron diffraction patterns of **5c**:PCBM blends from chloroform (CF) solvent in (A) as spun (AS), (B) annealed (Ann) films, and from chlorobenzene (CB) solvent in (C) as spun (AS), (D) annealed (Ann) films. GISAXS (E) and RSoXS (F) spectra of the blend films under different processing conditions.

was used as an electron donor to fabricate solution-processed BHJ cells with $PC_{61}BM$ and a PCE of 1.1% was obtained.[49] However, the devices based on the blend of **4**:$PC_{71}BM$ delivered better performance with a V_{oc} of 0.83 V, J_{sc} of 5.41 mA cm^{-2}, and fill factor of 0.41, leading to a PCE of ∼2%. Although this class of molecules shows significantly enhanced performance relative to the linear acenes due to the absence of Diels–Alder reactions with fullerenes, there is still a strong tendency to crystallize into well-defined large domains, reducing the donor–acceptor interfacial area and leading to a decrease in the photocurrent generating capacity of the blend due to exciton recombination.[50] Therefore, postdeposition methods are required to control the morphology. Our studies confirm that the processing solvents have a profound influence on the morphology of BHJ blends based on our acene materials (Figure 8).[51] When a less volatile solvent such as chlorobenzene is used, large crystalline domains are formed (∼80 nm), exceeding the length scale suitable for BHJ solar cells. In contrast, low boiling point solvents kinetically trap the morphology at a smaller length scale (∼50 nm) that is more favorable for charge separation. The thermal annealing process enhances the crystallinity of the acenes and improves the purity of PCBM domain, which likely lead to higher performance.

Although the power conversion efficiencies shown in initial device studies lag behind that of oligomer and polymer alternatives, these 2-D acenes show great potential with their strong intermolecular interactions for charge delocalization, high mobility, and good absorption. There is considerable room for further optimization of the device morphology by incorporation of different silylethynyl substituents and alternative processing conditions, including the use of solvent additives.

4. SUMMARY AND OUTLOOK

This Account summarized our recent efforts on chemically stable 2-D angular PAHs and their modern use in organic semiconductor-based devices. To improve chemical stability of PAHs, it is imperative to increase the aromatic stabilization energy of the core structure. This can be achieved by following the Clar sextet concept. Chemical stability and electronic structure determination of PAHs can be estimated by DFT calculations. Molecular geometries with large aspect ratios can provide dense crystal packing and large transfer integrals for high-performance devices. Importantly, PAHs with 2-D fused aromatic ring frameworks show greatly enhanced stability to oxygen and photo-oxidation, and have decreased Diels–Alder reactivity with fullerene derivatives. These molecules provide an excellent basis for exploring the properties and applications of larger acenes.

As the strategy used to create these molecules makes a second dimension synthetically accessible, the development of 2-D angular acenes with large aspect ratios (Figure 5) can be continued. Further systematic modification of the structure of these materials to tune their absorption, band structure, crystallinity, and electronic coupling will result in increased device performance in photovoltaics and transistors. Furthermore, due to the increased solubility of the 2-D acenes, they may find use as building blocks for low band gap copolymers. Our group is working toward these goals, and we hope that this Account encourages additional research exploring larger acenes and their applications in organic devices.

■ AUTHOR INFORMATION

Corresponding Author

*E-mail: abriseno@mail.pse.umass.edu.

Notes

The authors declare no competing financial interest.

Biographies

Lei Zhang completed his Ph.D. in Institute of Chemistry, CAS (ICCAS) with Prof. Zhaohui Wang. He is currently a postdoc in Conte Polymer Research Center, at UMass, Amherst. His research interests focus on design/synthesis of conjugated small molecules, oligomers, and polymers for organic devices.

Yang Cao received her B.S. in Physical Chemistry from University of Science and Technology of China in 2009 and recently obtained her Ph.D. degree at UCLA with K. N. Houk. Her research focuses on computational investigations of organic reactions on graphene, fullerenes, and self-assembled monolayers.

Nicholas S. Colella earned his B.A. in chemistry and mathematics from Williams College in 2009 and is currently a Ph.D. student in the department of Polymer Science & Engineering at UMass, Amherst. His research focuses on the crystallization of small molecule, oligomer, and polymer semiconductors.

Yong Liang received his B.S. (2005) and Ph.D. (2010) degrees at Peking University, working with Jiaxi Xu as an undergraduate and Zhi-Xiang Yu as a graduate student in the field of synthetic and computational organic chemistry. He is currently a postdoctoral scholar in the Houk research group at UCLA. His main research interest is to understand reaction mechanisms at the molecular level and controlling factors for the reactivity and selectivity of important chemical transformations.

Jean-Luc Brédas received his Ph.D. under the supervision Jean-Marie André at the University of Namur, Belgium, in 1979. He recently moved from the Georgia Institute of Technology to the King Abdullah University of Science and Technology in Thuwal, Saudi Arabia, where he is Distinguished Professor of Materials Science and Engineering and the Rawabi Holding Research Chair in Solar Energy Science and Engineering and serves as Director of the Solar & Photovoltaics Engineering Research Center. He is a member of the European Academy of Sciences, International Academy of Molecular Quantum Science, and Royal Academy of Belgium. His research interests focus on the theoretical understanding and design of novel organic materials for electronic and photonic applications.

K. N. Houk is the Saul Winstein Chair in Organic Chemistry at UCLA. He is a computational organic chemist. He received his Ph.D. with R. B. Woodward in 1968, at Harvard. He has published extensively on pericyclic reactions, stereoselectivity, molecular recognition, and enzyme design. He is a Fellow of the American Academy of Arts and Sciences, a member of the National Academy of Sciences, and a Senior Editor of this journal.

A. L. Briseno received his M.S. in chemistry at UCLA with Professor Fred Wudl in 2006. In 2008, he received his Ph.D. with Professors Y. Xia and S. Jenekhe at the University of Washington and was also coadvised by Professor Z. Bao while supported on a Bell Laboratories-Lucent Fellowship. He subsequently did a postdoc at UC Berkeley with Professor P. Yang. In 2009, he joined the Department of Polymer Science & Engineering at UMass Amherst. He is the recipient of the 3M Nontenured Award, the Office of Naval Research Young Investigator Program Award, the DOW Distinguished Lecturer at UCSB, the P&G Distinguished Lecturer at UCLA, and the Presidential Early Career Award for Scientists and Engineers (PECASE).

■ ACKNOWLEDGMENTS

Collaboration between the UMass (L.Z., A.L.B.) and Georgia Tech groups (J.L.B.) is supported by the Office of Naval Research awards N000141110636, N0001471410053, and N000141110211. N.S.C. was supported by the Center for Hierarchical Manufacturing, (CMMI-0531171). K.N.H. is grateful to the National Science Foundation (CHE-1059084 and CHE-1361104) for financial support and the Extreme Science and Engineering Discovery Environment (XSEDE) for computer support.

■ REFERENCES

(1) Clar, E. *The Aromatic Sextet*; Wiley-VCH: London, 1972.
(2) Haley, M. M., Tykwinski, R. R., Eds. *Carbon-Rich Compounds: From Molecules to Materials*; Wiley-VCH: Weinheim, 2006.
(3) Wu, J.; Pisula, W.; Müllen, K. Graphenes as Potential Material for Electronics. *Chem. Rev.* **2007**, *107*, 718−747.
(4) Bendikov, M.; Wudl, F.; Perepichka, D. F. Tetrathiafulvalenes, Oligoacenenes, and Their Buckminsterfullerene Derivatives: The Brick and Mortar of Organic Electronics. *Chem. Rev.* **2004**, *104*, 4891−4946.
(5) Anthony, J. E. Functionalized Acenes and Heteroacenes for Organic Electronics. *Chem. Rev.* **2006**, *106*, 5028−5048.
(6) Anthony, J. E. The Larger Acenes: Versatile Organic Semiconductors. *Angew. Chem., Int. Ed* **2008**, *47*, 452−483.
(7) Wei, J.; Yan, L.; Wang, Z. Heteroarenes as high performance organic semiconductors. *Chem. Soc. Rev.* **2013**, *42*, 6113−6127.
(8) Takimiya, K.; Osaka, I.; Mori, T.; Nakano, M. Organic Semiconductors Based on [1]Benzothieno[3,2-b][1]benzothiophene Substructure. *Acc. Chem. Res.* **2014**, *47*, 1493−1502.
(9) Zade, S. S.; Bendikov, M. Heptacene and Beyond: The Longest Characterized Acenes. *Angew. Chem. Int. Ed* **2010**, *49*, 4012−4015.
(10) Biermann, D.; Schmidt, W. Diels-Alder Reactivity of Polycyclic Aromatic Hydrocarbons. 1. Acenes and Benzologs. *J. Am. Chem. Soc.* **1980**, *102*, 3163−3173.
(11) Havey, R. G. *Polycyclic Aromatic hydrocarbons*; Wiley-VCH: New York, 1997.
(12) Schleyer, P. V. R.; Manoharan, M.; Jiao, H.; Stahl, F. The Acenes: Is There a Relationship between Aromatic Stabilization and Reactivity? *Org. Lett.* **2001**, *3*, 3643−3646.
(13) Ehrlich, S.; Bettinger, H. F.; Grimme, S. Dispersion-Driven Conformational Isomerism in σ-Bonded Dimers of Larger Acenes. *Angew. Chem., Int. Ed* **2013**, *52*, 10892−10895.
(14) Einholz, R.; Bettinger, H. F. Heptacene: Increased Persistence of a 4n+2 π-Electron Polycyclic Aromatic Hydrocarbon by Oxidation to the 4n π-Electron Dication. *Angew. Chem., Int. Ed* **2013**, *52*, 9818−9820.
(15) Zade, S. S.; Zamoshchik, N.; Reddy, A. R.; Marueli, G. F.; Sheberla, D.; Bendikov, M. Products and Mechanism of Acene Dimerization. A Computational Study. *J. Am. Chem. Soc.* **2011**, *133*, 10803−10806.
(16) Xiao, J.; Duong, H.; Liu, Y.; Shi, W.; Ji, L.; Li, G.; Li, S.; Liu, X.; Ma, J.; Wudl, F.; Zhang, Q. Synthesis and Structure Characterization of a Stable Nonatwistacene. *Angew. Chem., Int. Ed* **2012**, *51*, 6094−6098.
(17) Purushothaman, B.; Bruzek, M.; Parkin, S. R.; Miller, A.; Anthony, J. E. Synthesis and Structural Characterization of Crystalline Nonacenes. *Angew. Chem., Int. Ed* **2011**, *50*, 7013−7017.
(18) Kaur, I.; Jazdzyk, M.; Stein, N. N.; Prusevich, P.; Miller, G. P. Design, Synthesis, and Characterization of a Persistent Nonacene Derivative. *J. Am. Chem. Soc.* **2010**, *132*, 1261−1263.
(19) Chun, D.; Cheng, Y.; Wudl, F. The Most Stable and Fully Characterized Functionalized Heptacene. *Angew. Chem., Int. Ed* **2008**, *47*, 8380−8385.
(20) Payne, M. M.; Parkin, S. R.; Anthony, J. E. Functionalized Higher Acenes: Hexacene and Heptacene. *J. Am. Chem. Soc.* **2005**, *127*, 8028−8029.
(21) Debije, M. G.; Piris, D.; de Haas, M. P.; Warman, J. M.; Tomović, Z.; Simpson, C. D.; Watson, M. D.; Müllen, K. The Optical and Charge Transport Properties of Discotic Materials with Large Aromatic Hydrocarbon Cores. *J. Am. Chem. Soc.* **2004**, *126*, 4641−4645.
(22) Clar, E. *Polycyclic Hydrocarbons*; Academic Press: New York, 1964; Vol. *1*.
(23) Suresh, C. H.; Gadre, S. R. Clar's Aromatic Sextet Theory Revisited via Molecular Electrostatic Potential Topography. *J. Org. Chem.* **1999**, *64*, 2505−2512.
(24) Pérez, D.; Peña, D.; Guitián, E. Aryne Cycloaddition Reactions in the Synthesis of Large Polycyclic Aromatic Compounds. *Eur. J. Org. Chem.* **2013**, 5981−6013.
(25) Chen, L.; Hernandez, Y.; Feng, X.; Müllen, K. From Nanographene and Graphene Nanoribbons to Graphene Sheets: Chemical Synthesis. *Angew. Chem., Int. Ed* **2012**, *51*, 7640−7654.
(26) Fudickar, W.; Linker, T. Why Triple Bonds Protect Acenes from Oxidation and Decomposition. *J. Am. Chem. Soc.* **2012**, *134*, 15071−15082.

(27) Northrop, B. H.; Houk, K. N.; Maliakal, A. Photostability of Pentacene and 6,13-Disubstituted Pentacene Derivatives: A Theoretical and Experimental Mechanistic Study. *Photochem. Photobiol. Sci.* **2008**, *7*, 1463−1468.
(28) Tsefrikas, V. M.; Scott, L. T. Geodesic Polyarenes by Flash Vacuum Pyrolysis. *Chem. Rev.* **2006**, *106*, 4868−4884.
(29) Yang, C.; Harvey, R. G. Synthesis of Methylene-Bridged Polycyclic Aromatic Hydrocarbons. *J. Org. Chem.* **1993**, *58*, 4155−4158.
(30) Zhang, X.; Li, J.; Qu, H.; Chi, C.; Wu, J. Fused Bispentacenequinone and Its Unexpected Michael Addition. *Org. Lett.* **2010**, *12*, 3946−3949.
(31) Zhang, L.; Fonari, A.; liu, Y.; Hoyt, A.; Lee, H.; Granger, D.; Parkin, S.; Russell, T. P.; Anthony, J. E.; Brédas, J. L.; Coropceanu, V.; Briseno, A. L. Bistetracene: An Air-Stable, High-Mobility Organic Semiconductor with Extended Conjugation. *J. Am. Chem. Soc.* **2014**, *136*, 9248−9251.
(32) Wiberg, K. B. Properties of Some Condensed Aromatic Systems. *J. Org. Chem.* **1997**, *62*, 5720−5727.
(33) Purushothaman, B.; Parkin, S. R.; Anthony, J. E. Synthesis and Stability of Soluble Hexacenes. *Org. Lett.* **2010**, *12*, 2060−2063.
(34) Zhang, L.; Fonari, A.; Zhang, Y.; Zhao, G.; Coropceanu, V.; Hu, W.; Parkin, S.; Brédas, J. L.; Briseno, A. L. Triisopropylsilylethynyl-Functionalized Graphene-Like Fragment Semiconductors: Synthesis, Crystal Packing, and Density Functional Theory Calculations. *Chem.—Eur. J.* **2013**, *19*, 17907−17916.
(35) Miller, G. P.; Mack, J. Completely Regioselective, Highly Stereoselective Syntheses of cis-Bisfullerene[60] Adducts of 6,13-Disubstituted Pentacenes. *Org. Lett.* **2000**, *2*, 3979−3982.
(36) Lloyd, M. T.; Anthony, J. E.; Malliaras, G. G. Photovoltaics from Soluble Small Molecules. *Mater. Today* **2007**, *10*, 34−41.
(37) Cao, Y.; Liang, Y.; Zhang, L.; Osuna, S.; Hoyt, A-L. M.; Briseno, A. L.; Houk, K. N. Why Bistetracenes Are Much Less Reactive than Pentacenes in Diels-Alder Reactions with Fullerenes. *J. Am. Chem. Soc.* **2014**, *136*, 10743−10751.
(38) Desiraju, G. R.; Gavezzotti, A. A Systematic Analysis of Packing Energies and Other Packing Parameters for Fused-Ring Aromatic Hydrocarbons. *Acta Crystallogr. B* **1988**, *44*, 427−434.
(39) Zhong, J.; Munakata, M.; Kuroda-Sowa, T.; Maekawa, M.; Suenaga, Y.; Konaka, H. Spiral, Herringbone, and Triple-Decker Silver(I) Complexes of Benzopyrene Derivatives Assembled through η^2-Coordination. *Inorg. Chem.* **2001**, *40*, 3191−3199.
(40) Sherrill, C. D. Energy Component Analysis of π Interactions. *Acc. Chem. Res.* **2013**, *46*, 1020−1028.
(41) Brédas, J. L.; Calbert, J. P.; da Silva Filho, D. A.; Cornil, J. Organic Semiconductors: A Theoretical Characterization of the Basic Parameters Governing Charge Transport. *Proc. Natl. Acad. Sci. U.S.A.* **2002**, *99*, 5804−5809.
(42) Burke, K. B.; Shu, Y.; Kemppinen, P.; Singh, B.; Bown, M.; Liaw, I. I.; Williamson, R. M.; Thomsen, L.; Dastoor, P.; Belcher, W.; Forsyth, C.; Winzenberg, K. N.; Collis, G. E. Single Crystal X-ray, AFM, NEXAFS, and OFET Studies on Angular Polycyclic Aromatic Silyl-Capped 7,14-Bis(ethynyl)dibenzo[b,def]chrysenes. *Cryst. Growth Des* **2012**, *12*, 725−731.
(43) Shu, Y.; Collis, G. E.; Dunn, C. J.; Kemppinen, P.; Winzenberg, K. N.; Williamson, R. M.; Bilic, A.; Birendra Singh, T.; Bown, M.; McNeillc, C. R.; Thomsenb, L. The impact of Tetrahedral Capping Groups and Device Processing Conditions on the Crystal Packing, Thin Film Features and OFET Hole Mobility of 7,14-Bis(ethynyl)-dibenzo[*b,def*]chrysenes. *J. Mater. Chem. C* **2013**, *1*, 6299−6307.
(44) Coropceanu, V.; Cornil, J.; da Silva Filho, D. A.; Olivier, Y.; Silbey, R.; Brédas, J. L. Charge Transport in Organic Semiconductors. *Chem. Rev.* **2007**, *107*, 926−952.
(45) Goldman, C.; Haas, S.; Krellner, C.; Pernstich, P.; Gundlach, D. J.; Batlogg, B. Hole Mobility in Organic Single Crystals Measured by a "Flip-Crystal" Field-Effect Technique. *J. Appl. Phys.* **2004**, *96*, 2080−2086.
(46) Watanabe, M.; Chang, Y.; Liu, S.; Chao, T.; Goto, K.; Minarul Islam, M.; Yuan, C.; Tao, Y.; Shinmyozu, T.; Chow, T. J. The synthesis, Crystal Structure and Chargetransport Properties of Hexacene. *Nat. Chem.* **2012**, *4*, 575−578.
(47) Winzenberg, K. N.; Kemppinen, P.; Fanchini, G.; Bown, M.; Collis, G. E.; Forsyth, C. M.; Hegedus, K.; Singh, Th. B.; Watkins, S. E. Dibenzo[b,def]chrysene Derivatives: Solution-Processable Small Molecules that Deliver High Power-Conversion Efficiencies in Bulk Heterojunction Solar Cells. *Chem. Mater.* **2009**, *21*, 5701−5703.
(48) Scholes, F. H.; Ehlig, T.; James, M.; Lee, K. H.; Duffy, N.; Scully, A. D.; Singh, T. B.; Winzenberg, K. N.; Kemppinen, P.; Watkins, S. E. Intraphase Microstructure−Understanding the Impact on Organic Solar Cell Performance. *Adv. Funct. Mater.* **2013**, *23*, 5655−5662.
(49) Zhang, L.; Walker, B.; Liu, F.; Colella, N. S.; Mannsfeld, S. C. B.; Watkins, J. J.; Nguyen, T.-Q.; Briseno, A. L. Triisopropylsilylethynyl-Functionalized Dibenzo[*def,mno*]chrysene: A Solution-Processed Small Molecule for Bulk Heterojunction Solar Cells. *J. Mater. Chem.* **2012**, *22*, 4266−4268.
(50) Walker, B.; Kim, C.; Nguyen, T.-Q. Small Molecule Solution-Processed Bulk Heterojunction Solar Cells. *Chem. Mater.* **2011**, *23*, 470−482.
(51) Liu, F.; Zhang, L.; Zhang, Y.; Mannsfeld, S. C. B.; Russell, T. P.; Briseno, A. L. Interpenetrating Morphology based on Highly Crystalline Small Molecule and PCBM Blends. *J. Mater. Chem. C* **2014**, *2*, 9368−9374.